Met. Mater. Int., Vol. 18, No. 6 (2012), pp. 933~938
doi: 10.1007/s12540-012-6004-5

Physical and Mechanical Properties of Al–Si–Ni Eutectic Alloy

Uğur Böyük*

Department of Science Education, Education Faculty, Erciyes University, Kayseri, Turkey

(received date: 12 October 2011 / accepted date: 25 January 2012)

Al–11.1wt%Si–4.2wt%Ni alloy was directionally solidified upward under different conditions, with different growth rates (V=4.60–243.33 μm/s) at a constant temperature gradient (G=5.82 K/mm) and with different temperature gradients (G=2.11–5.82 K/mm) at a constant growth rate (V=11.63 μm/s) by using a Bridgman type directional solidification furnace. The microstructure of directionally solidified Al–11.1wt%Si–4.2wt%Ni alloy was observed to be irregular plates of Al_3Ni and Si within an α–Al matrix from quenched samples. The microhardness, tensile strength and electrical resistivity of the alloy were measured from directionally solidified samples. The dependency of the microhardness, tensile strength and electrical resistivity for directionally solidified Al–Si–Ni eutectic alloy on the solidification parameters were investigated and the relationships between them were experimentally obtained by using regression analysis. Additionally, the variation of electrical resistivity with temperature in the range of 300-825 K for the Al–Si–Ni eutectic cast alloy was also measured using a standard d.c. four-point probe technique. The enthalpy of fusion and specific heat for the same alloy were determined by a differential scanning calorimeter from the heating curve during the transformation from eutectic solid to eutectic liquid. The results obtained in the present work were compared with previous similar experimental results.

Key words: solidification, alloys, mechanical properties, tensile test, hardness test

1. INTRODUCTION

Solidification and melting are transformations between the crystallographic and non-crystallographic states of a metal or alloy. These transformations are basic to such technological applications as ingot and continuous casting, and directional solidification of composites and single crystals. An understanding of the mechanism of solidification and how it is affected by such parameters as temperature distribution, solidification condition and alloying, are important in the control of the mechanical and electrical properties of cast metals and fusion welds [1].

Unidirectional solidification of eutectic alloys has received considerable attention in the past few years because the alignment of fibers or plates in some of these eutectics produces attractive directional physical or mechanical properties. Most of the work has been done on binary alloys of eutectic and near eutectic compositions, and only recently work has been initiated in the area of ternary eutectic alloys [2].

More recently, Al–based alloys with high strength and light weight have attracted rapidly increasing interest because of the increase in the importance of energy and environmental problems on the earth. Ordinary Al–based alloys have been developed using the following conventional strengthening mechanisms; *i.e.*, solid solution, precipitation, grain size refinement, dispersion, work hardening and fiber reinforcement [3]. Multicomponent Al–Ni–Si based alloys are used for a variety of engineering applications due to their interesting properties such as good castability, high strength, light weight, good wear resistance and low thermal expansion [4–8].

The purpose of the present work was to investigate the mechanical, electrical and thermal properties of Al–11.1 wt%Si–4.2 wt%Ni alloy. For this purpose, the dependency of microhardness (HV), tensile strength (σ_t) and electrical resistivity (ρ) on the solidification processing parameters (G and V) for directionally solidified Al–11.1 wt%Si–4.2 wt%Ni alloy, and electrical resistivity on temperature ranging from 300-825 K for Al–11.1 wt%Si–4.2 wt%Ni cast alloy, were investigated. Enthalpy of fusion (ΔH) and specific heat (C_p) for the same alloy were also determined from the heating curve during the transformation from eutectic solid to eutectic liquid.

2. EXPERIMENTAL PROCEDURES

In the present work, the experimental procedure consists of alloy preparation, measurements of the microhardness, tensile strength and electrical resistivity of the directionally solidified Al–11.1 wt%Si–4.2 wt%Ni alloy, and determina-

*Corresponding author: boyuk@erciyes.edu.tr

tion of the variation of electrical resistivity with temperature, enthalpy of fusion and the specific heat for Al–11.1 wt%Si–4.2 wt%Ni cast.

2.1. Alloy preparation and directional solidification

Using a vacuum melting furnace and a hot filling furnace, Al–11.1 wt%Si–4.2 wt%Ni eutectic alloy was prepared under vacuum atmosphere by melting aluminum, silicon and nickel of high purity (>99.9%). After allowing time for melting homogenization, the molten alloy was poured into 12 graphite crucibles (200 mm in length 4 mm ID and 6.35 mm OD) held in a specially constructed casting furnace (Hot Filling Furnace) at approximately 50 K above the melting point of the alloy. The molten alloy was directionally solidified from bottom to top to ensure that the crucible was completely full.

Solidification of the Al–Si–Ni eutectic alloy was carried out with different growth rates (V=4.60–243.33 mm/s) at a constant temperature gradient (G=5.82 K/mm) and with different temperature gradients (G=2.11–5.82 K/mm) at a constant growth rate (V=11.63 μm/s) in the Bridgman-type growth apparatus. The temperature of water in the reservoir was kept at 283 K to an accuracy of ±0.01 K using a Poly Science digital 9102 model heating / refrigerating circulating bath to get a well quenched solid-liquid interface. The temperature in the sample was also controlled to an accuracy of ±0.1 K degrees with a Eurotherm 2604 type controller. The details of the apparatus and experimental procedures are given in Refs. [9-10]. The quenched samples were removed from the graphite crucible and cut into lengths of typically 3 mm. After the metallographic process, the microstructures of the samples were revealed.

The cooling rate was so slow that it could be considered an equilibrium solidification process, which corresponds to an eutectic reaction: L→Al_3Ni+Si+α-Al. The quantitative chemical composition analysis of irregular plates of Al_3Ni and Si and α-Al matrix were carried out by using energy dispersive X-ray analysis (EDX). According to EDX results, grey, black and white phases were identified as plates of Al_3Ni and Si and α-Al matrix, respectively. Typical optical images of growth morphologies of directionally solidified Al–11.1 wt%Si–4.2 wt%Ni alloy are shown in Fig. 1.

2.2. The measurement of microhardness

One of the purposes of this investigation was to learn the relationships between the solidification processing parameters, and microhardness, for directionally solidified Al-Ni-Si eutectic alloy. The mechanical properties of any solidified materials are usually determined with a hardness test, tensile strength test, etc. The Vickers hardness (HV) is the ratio of a load applied to the indenter to the surface area of the indentation. This is given by

$$HV = \frac{2P\sin(\theta/2)}{d^2} \quad (1)$$

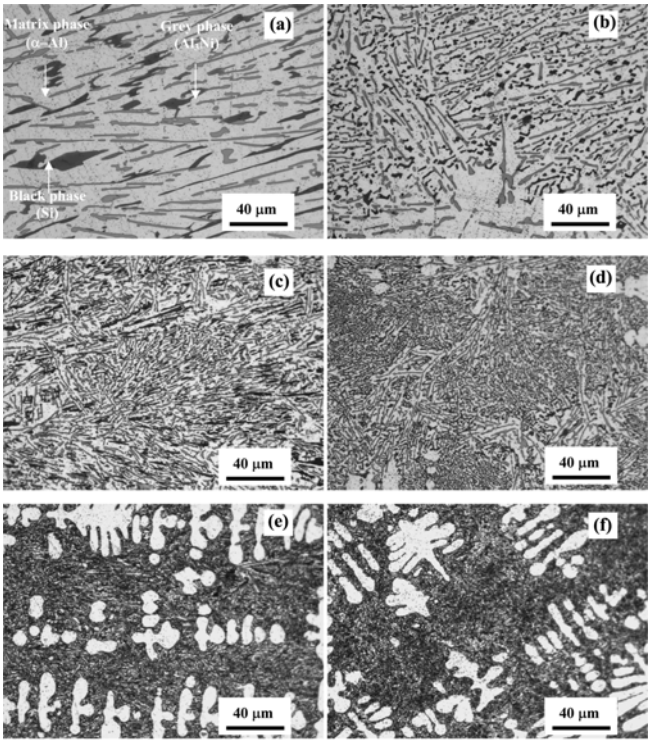

Fig. 1. Typical optical images of the growth morphologies of directionally solidified Al–11.1 wt%Si–4.2 wt%Ni eutectic alloy. (a) Longitudinal section, (b) transverse section (V=4.60 μm/s, G=5.82 K/mm), (c) longitudinal section, (d) transverse section (V=35.14 μm/s, G=5.82 K/mm), (e) longitudinal section, and (f) transverse section (V=243.33 μm/s, G=5.82 K/mm).

where HV is the Vickers microhardness in kg/mm^2, P is the applied load (kg), d is the mean diagonal of the indentation (mm), θ is the angle between opposite faces of the diagonal indenter (136°). Microhardness measurements in this present work were made with a Future-Tech FM-700 model hardness measuring test device using a 500 g load and a dwell time of 10 s, giving a typical indentation depth of about 40-60 μm, which is significantly smaller than the original solidified samples. Microhardness is the average of at least 30 measurements on the transverse sections (HV). Variations of microhardness with growth rate and temperature gradient for the Al–Si–Ni eutectic alloy are plotted in Figs. 2 and 3, respectively, and compared with the previous experimental results for binary Al–Si [11] and Al–Ni [12] eutectic alloys.

2.3. Measurement of tensile strength

The uniaxial tensile test was performed at room temperature at a strain rate of 10^{-3} s^{-1} with a Shimadzu Universal Testing Instrument (Type AG–10KNG), which was designed for testing the stress–strain responses of solders. In order to avoid damaging the sample surface, two seals were stuck on the sample instead of the traditional clip gauge. Strains were

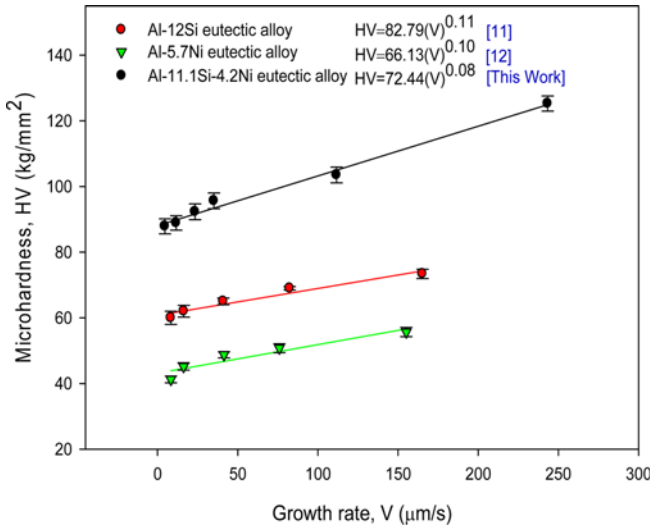

Fig. 2. Variation of microhardness, as a function of growth rate for directionally solidified Al–Si–Ni eutectic alloy at a constant temperature gradient, and compared with the binary Al–Si and Al–Ni eutectic alloys.

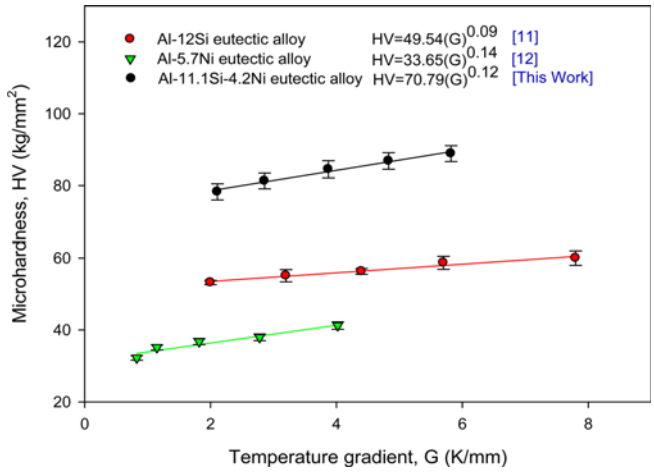

Fig. 3. Variation of microhardness, as a function of temperature gradient for directionally solidified Al–Si–Ni eutectic alloy at a constant growth rate, and compared with the binary Al–Si and Al–Ni eutectic alloys.

then measured by observing the displacement between the two seals using a video camera. A computer with data acquisition software was used to collect the data. The data collected from the tensile test can be analyzed using the following formula to determine the strength (σ).

$$\sigma = \frac{F}{A} \tag{2}$$

where σ is the strength in N/mm^2 (or MPa), F is the applied force (N), A is the original cross sectional area (mm^2) of the sample. Round rod tensile samples with a diameter of 4 mm and gauge length of 20 mm were prepared from directionally solidified rod samples with different solidification

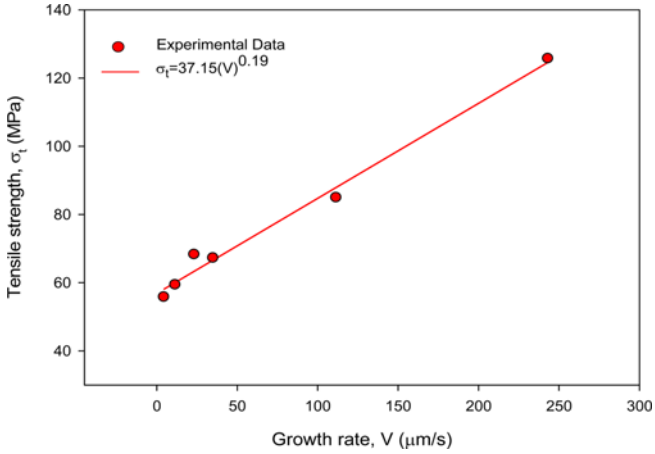

Fig. 4. Variation of tensile strength, as a function of growth rate for directionally solidified Al–Si–Ni eutectic alloy at a constant temperature gradient.

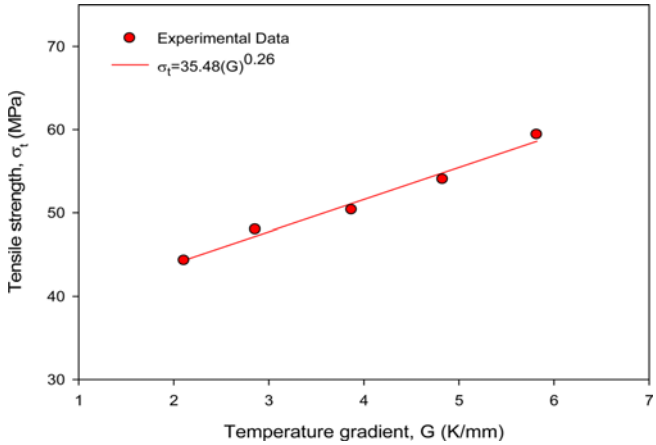

Fig. 5. Variation of tensile strength, as a function of temperature gradient for directionally solidified Al–Si–Ni eutectic alloy at a constant growth rate.

parameters. The tensile axis was chosen parallel to the growth direction of the sample and the tests were repeated three times. Variations of tensile strength with growth rate and temperature gradient for the Al–Si–Ni eutectic alloy are plotted in Figs. 4 and 5, respectively. As can be seen from Figs. 4 and 5, the values of tensile strength for the Al–Si–Ni eutectic alloy increase with increasing values of V and G.

2.4. The measurement of electrical resistivity

Electrical resistivity is an imperative physical property. Impurities observed in metals distort the metal lattice and can affect the behavior of ρ to a considerable extent. This is particularly true for metal alloys. The value of electrical resistivity is also affected by grain size (*e.g.*, higher ρ corresponds to finer grain), plastic deformation, heat treatment, and some other factors, but to a smaller extent compared to the effect of temperature and chemical composition [13].

The growth rate, temperature gradient and temperature dependence of electrical resistivity for Al-Ni-Si alloys was measured by the four-point probe method [14]. A Keithley 2400 sourcemeter was used to provide constant current, and the potential drop was measured by a Keithley 2700 multimeter through an interface card, which was controlled by a computer. Platinum wires with a diameter of 0.5 mm were used as current and potential probes. The voltage drop was detected, and electrical resistivity and conductivity were determined using a standard conversion method.

Firstly, the electrical resistivities of the directionally solidified Al–Si–Ni eutectic alloys were measured by the d.c. four-point probe method at room temperature. Secondly, the temperature dependence of the electrical resistivity for casting of Al–Si–Ni eutectic alloy was measured. Temperature dependent measurements were made in the temperature range of 300-825 K. The temperature of the sample was adjusted by a controllable Nabertherm P320 heater, and the temperature of the sample was measured using a standard K–type thermocouple which was placed near the samples.

Variations of electrical resistivity with growth rate, temperature gradient and temperature for the Al–Si–Ni eutectic alloy are plotted in Figs. 6, 7 and 8, respectively. It can be seen from Figs. 6-8, the values of electrical resistivity for the Al–Si–Ni eutectic alloy increase with increasing values of V, G and T.

2.5. The measurements of thermal properties

Other purposes of the present work were to determine the enthalpy of fusion and specific heat for the Al-Ni-Si cast. Enthalpy of fusion and specific heat of Al-Ni-Si eutectic alloys were measured because they are very important parameters for industrial applications. A DSC (Perkin Elmer Diamond model) thermal analysis was performed in the temperature range of 300-1100 K with a heating rate of 10 K/min and under a constant stream of nitrogen at atmospheric pressure. The DSC curve obtained for Al-Ni-Si eutectic alloy is shown in Fig. 9. Clearly, a sharp peak is observed for the melting process as shown in Fig. 9. The enthalpy of fusion and specific heat were calculated by numerical integration as the area under the peak.

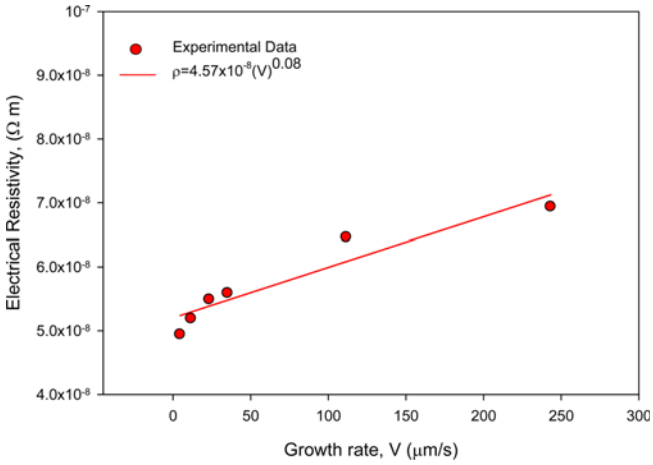

Fig. 6. Variation of electrical resistivity, as a function of growth rate for directionally solidified Al–Si–Ni eutectic alloy at a constant temperature gradient.

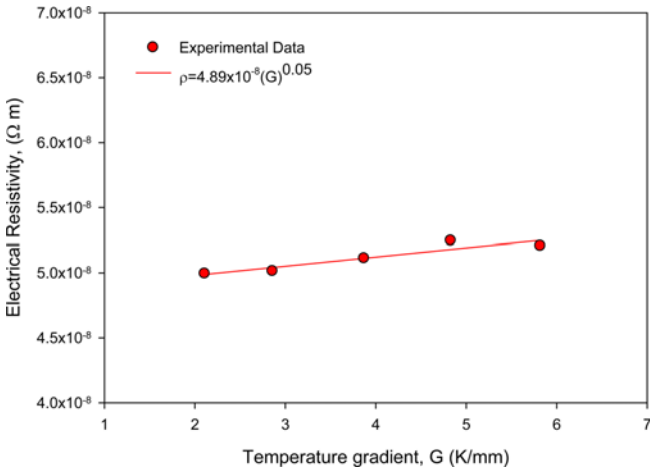

Fig. 7. Variation of electrical resistivity, as a function of temperature gradient for directionally solidified Al–Si–Ni eutectic alloy at a constant growth rate.

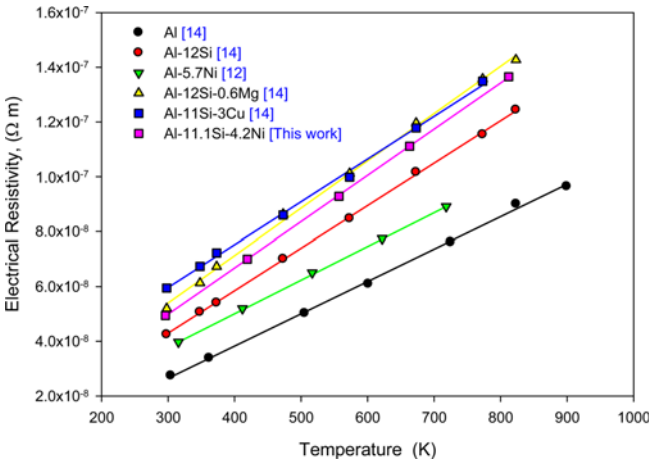

Fig. 8. Temperature dependence of the electrical resistivity for Al, and Al–rich alloys.

3. RESULTS AND DISCUSSION

3.1. The effect of solidification parameters on microhardness

It can also be seen from Figs. 2 and 3 that an increase in solidification parameters leads to an increase in the HV. The dependence of the HV on V and G were determined by linear regression analysis and the relationship between them can be expressed as:

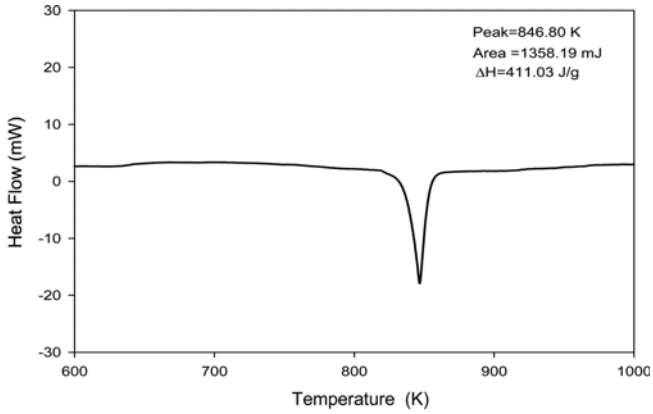

Fig. 9. Heat flow versus temperature for Al–Si–Ni eutectic alloy with a heating rate of 10 K/min.

$$HV = k_1(V)^a \tag{3}$$

$$HV = k_2(G)^b \tag{4}$$

where k is a constant, a and b are the exponent values relating to the growth rate and temperature gradient respectively.

Figure 2 shows the variation of HV as a function of V at a constant G. The value of HV increases with the increasing value of V. The relationship between the HV and V was determined to be HV=72.44(V) for Al-Ni-Si eutectic alloy by using linear regression analysis. This exponent value (0.08) agrees with the exponent values of V (0.07-0.11) obtained by various researchers [15-20] for different binary and ternary eutectic alloy systems, under similar solidification conditions.

Dependency of HV on the temperature gradient (G) for unidirectional solidified Al-Ni-Si eutectic alloy was also determined as HV=72.44$(G)^{0.12}$. It can be seen from Fig. 3, the value of microhardness also increases with the increasing value of the temperature gradient for a given growth rate (V). This exponent value relating to G obtained in the present work is generally in good agreement with the exponent values relating to the G (0.11-0.19) obtained in previous experimental works [20-23] for different binary and ternary eutectic alloy systems.

The exponent values of HV relating to growth rate and temperature gradient for directionally solidified Al–Si–Ni eutectic alloy obtained in the present work are slightly higher than the exponent values of HV relating to V and G for the Al–Si [11] and Al–Ni [12] eutectic alloys, solidified under similar conditions.

3.2. The effect of solidification parameters on tensile strength

Figures 4 and 5 show the variation of tensile strength values (σ_t) with growth rate and temperature gradient. The dependence of σ_t on the V and G can be represented by equations as follows:

$$\sigma_t = k_3(V)^m \tag{5}$$

$$\sigma_t = k_4(G)^n \tag{6}$$

where k is a constant, m and n are the exponent values relating to the growth rate and temperature gradient, respectively.

From Fig. 4, by using linear regression analysis, the relationship between σ_t and V was found to be $\sigma_t = 37.15(V)^{0.19}$ and it can also be seen that values of the tensile strength increase with increasing growth rate. It was found that an increase in growth rate from 4.6 μm/s to 243.33 μm/s, increases the tensile strength from 55.71 to 125.62 MPa. It appears that the size of the Si and $A1_3Ni$ phases governs the properties, and the slight alignment of colonies due to unidirectional solidification is masked by the particle size effect. A leading phase, (Si or Al3Ni platelets) in the ternary eutectic appears to be changed into microstructure, increasing the growth rates as shown in Figs. 1(e) and (f). Therefore, microstructure is considered to enhance the tensile strength.

The maximum and minimum values of σ_t for A1–Si–Ni eutectic alloy are smaller than the maximum and minimum values of σ_t obtained by Rohatgi *et al*. [2] for unidirectional solidified Al–Si–Ni (138 MPa for 5.56 μm/s and 157 MPa for 6.95 μm/s) eutectic alloy. Besides, the tensile strengths of unidirectional solidified A1–Si–Ni eutectics are lower than those of the chill cast alloys [2].

Figure 5 shows the experimental results of tensile strength as a function of the temperature gradient. It can be seen that value of the tensile strength also increases with increasing temperature gradient. It was found that increasing the temperature gradient from 2.11 K/mm to 5.82 K/mm, increases the tensile strength from 44.31 to 59.38 MPa. Using linear regression analysis, the relationship between σ_t and G was found to be $\sigma_t = 35.48(G)^{0.26}$.

3.3. The effect of solidification parameters and temperature on electrical resistivity

Figures 6 and 7 show the variation of the electrical resistivity values with growth rate and temperature gradient. The dependence of ρ on the V and G can be represented by equations as follows:

$$\rho = k_5(V)^e \tag{7}$$

$$\rho = k_6(G)^f \tag{8}$$

where k is a constant, e and f are the exponent values relating to the growth rate and temperature gradient, respectively.

From Figs. 6 and 7, by using linear regression analysis the

relationships between ρ and V, ρ and G were found to be $\rho = 4.57\times10^{-8}(V)^{0.08}$ and $\rho = 4.89\times10^{-8}(G)^{0.05}$ and it can also be seen that values of the electrical resistivity increase with increasing growth rate and temperature gradient.

As mentioned above, the variation in electrical resistivity with temperature in the range of 300-825 K for Al-Ni-Si eutectic cast was measured, and plotted in Fig. 8. As can be seen from Fig. 8, the electrical resistivity of Al-Ni-Si eutectic cast increases linearly with increasing temperature. The result was compared with the values of ρ for pure Al and Al–based binary and ternary alloys as shown in Fig. 8. It can be seen from Fig. 8, the line of resistivity versus temperature for Al-Ni-Si eutectic cast is above the lines of resistivity versus temperature for pure Al and Al–Ni and Al–Si eutectic alloys, but fairly close to the lines of resistivity versus temperature for Al–based ternary alloys. This difference between them might be due to composition differences *i.e.* the composition of the alloy might have an effect on the electrical resistivity.

3.4. Determination of fusion enthalpy and specific heat

Al-Ni-Si eutectic alloy was heated with a heating rate of 10 K/min from room temperature to 1100 K by using a Perkin Elmer Diamond model DSC, and its heat flow versus temperature is given in Fig. 9. The melting temperature of Al-Ni-Si eutectic alloy was detected to be 837.73 K. The value of the enthalpy of fusion (ΔH) and specific heat (C_p) for Al-Ni-Si eutectic alloy were also calculated from the graph of the heat flow versus temperature, and found to be 411.03 J/g, and 0.716 J/g K, respectively.

4. CONCLUSIONS

In the present work, the influence of solidification processing parameters and temperature on the mechanical, electrical and thermal properties of Al–11.1wt%Si–4.2wt%Ni eutectic alloy were investigated. The results are summarized as follows.

(1) Values of microhardness increase with increasing values of V and G. The established relationships among HV, V and G can be given as $HV = 72.44(V)^{0.08}$ and $HV = 70.79(V)^{0.12}$.

(2) The experimental expressions correlating the values of σ_t with the values of V and G for directional solidified Al–Si–Ni eutectic alloy have shown that the values of the tensile strengths increase with increasing values of V and G. The established relationships among strengths and solidification parameters can be given as $\sigma_t = 37.15(V)^{0.19}$ and $\sigma_t = 35.48(G)^{0.26}$.

Values of electrical resistivity increase with increasing values of V and G. The established relationships among electrical resistivity and solidification parameters can be given as $\rho = 4.57\times10^{-8}(V)^{0.08}$ and $\rho = 4.89\times10^{-8}(G)^{0.05}$.

The molten Al–Si–Ni eutectic alloy was heated at a heating rate of 10 K/min from 300 K to 1100 K. From the trace of heat flow versus temperature, the melting temperature of Al–Si–Ni eutectic alloy was detected to be 837.73 K. The values of the enthalpy of fusion and the specific heat were found to be 411.03 J/g, and 0.716 J/g K, respectively.

REFERENCES

1. D. A. Porter and K. E. Easterling, *Phase Transformations in Metals and Alloys*, *2nd ed*, p.185, CRC Press, UK (1992).
2. P. K. Rohatgi, R. C. Sharma, and K. V. Prabhakar, *Metall. Mater. Trans. A* **6**, 569 (1975).
3. S. K. Seo, M. G. Cho, W. K. Choi, and H. M. Lee, *J. Electron. Mater.* **35**, 1975 (2006).
4. D. H. Kim, M. G. Cho, S. K. Seo, and H. M. Lee, *J. Electron. Mater.* **38**, 39 (2009).
5. M. G. Cho, S. K. Kang, D. Y. Shih, and H. M. Lee, *J. Electron. Mater.* **36**, 1501 (2007).
6. S. K. Kang, M. G. Cho, D. Y. Shih, S. K. Seo, and H. M. Lee, *Proc. 58th Electronic Components and Technology Conf.*, p. 478, Piscataway NJ:IEEE, USA (2008).
7. S. K. Seo, M. G. Cho, and H. M. Lee, *J. Electron. Mater.* **36**, 1536 (2007).
8. M. Abtew and G. Selvaduray, *Mater. Sci. Eng.* **27**, 95 (2000).
9. M. Gündüz, H. Kaya, E. Çadırlı, and A. Özmen, *Mater. Sci. Eng. A* **369**, 215 (2004).
10. U. Böyük, N. Maraşlı, H. Kaya, E. Çadırlı, and K. Keşlioğlu, *Appl. Phys. A-Mater.* **95**, 923 (2009).
11. H. Kaya, E. Çadırlı, M. Gündüz, and A. Ülgen, *J. Mater. Eng. and Perf.* **12**, 544 (2003).
12. H. Kaya, U. Böyük, E. Çadırlı, and N. Maraşlı, *Mater. Design* **34**, 707 (2012).
13. V. Rudnev, D. Loveless, R. Cook, and M. Black, *Handbook of Induction Heating*, p.119, Markel Dekker Inc., USA. (2003).
14. F. M. Smiths, *The Bell Sys. Tech. J.* **37**, 711 (1958).
15. F. Vnuk, M. Sahoo, R. Van De Merwe, and R. W. Smith, *J. Mater. Sci.* **14**, 975 (1979).
16. F. Vnuk, M. Sahoo, D. Baragor, and R. W. Smith, *J. Mater. Sci.* **15**, 2573 (1980).
17. A. I. Telli and S. E. Kısakürek, *Mater. Sci. Tech.* **4**, 153 (1988).
18. E. Çadırlı, U. Böyük, H. Kaya, N. Maraşlı, K. Keşlioşlu, S. Akbulut, and Y. Ocak, *J. Alloy. Compd.* **470**, 150 (2009).
19. U. Böyük and N. Maraşlı, *J. Alloy. Compd.* **485**, 264 (2009).
20. E. Çadırlı, U. Böyük, S. Engin, H. Kaya, and N. Marasli, *Kovove Mater.* **47**, 381 (2009).
21. H. Kaya, E. Çadırlı, U. Böyük, and N. Maraşlı, *App. Surf. Sci.* **255**, 3071 (2008).
22. H. Kaya, U. Böyük, E. Çadırlı Y. Ocak, S. Akbulut, K. Keşlioşlu, and N. Maraşlı, *Met. Mater. Int.* **14**, 575 (2008).
23. U. Böyük and N. Maraşlı, *Mater. Chem. Phys.* **119**, 442 (2010).
24. R. Brandt and G. Neuer, *Int. J. Thermophys.* **28**, 1429 (2007).